Lyapunov Spectrum and the Conjugate Pairing Rule for a Thermostatted Random Lorentz Gas: Numerical Simulations

Ch. Dellago and H. A. Posch

Institut für Experimentalphysik, Universität Wien, Boltzmanngasse 5, A-1090 Wien, Austria

(Received 26 September 1996)

We report on the numerical computation of the Lyapunov exponents and the Kolmogorov-Sinai entropy for a three-dimensional, dilute, random Lorentz gas both in equilibrium and in nonequilibrium steady states. In our method the phase- and tangent-space dynamics are treated exactly. Furthermore, we propose a highly efficient stochastic technique for the computation of Lyapunov spectra of dilute systems. Our results are in excellent agreement with analytical results of Latz, van Beijeren, and Dorfman [preceding Letter, Phys. Rev. Lett. **78**, 207 (1997)]. [S0031-9007(96)02159-X]

PACS numbers: 05.45.+b, 02.70.Ns, 05.20.–y

The field driven Lorentz gas is, arguably, the simplest model which still displays all the features characteristic for thermostatted nonequilibrium steady states [1,2]. Although its dynamics is governed by time-reversible equations of motion, any phase-space volume element is continuously shrinking, and the invariant phase-space distribution collapses onto a multifractal strange attractor with information dimension strictly less than the phase space dimension. Nevertheless, the system is ergodic in the sense that a typical trajectory comes arbitrarily close to every point of the accessible phase space.

Recently, van Beijeren and Dorfman [3] used methods based on the Boltzmann equation to derive analytical expressions for the Lyapunov exponents of the dilute two-dimensional Lorentz gas in equilibrium. Their method was subsequently extended to treat also weak nonequilibrium steady states [4]. In the preceding Letter, Latz, van Beijeren, and Dorfman [5] succeeded in generalizing this kinetic theory to derive analytical expressions for the full spectrum of Lyapunov exponents of the dilute, three-dimensional, driven Lorentz gas up to second order in the applied field. To complement these results we present in this Letter numerical simulations of the full Lyapunov spectrum and the Kolmogorov-Sinai entropy for the same model.

The random Lorentz gas considered here consists of a point particle with mass m and charge q, moving in an infinite, three-dimensional, random array of nonoverlapping scatterers. The scatterers are hard spheres with radius a, on which the moving particle is elastically reflected. An external field $\vec{E}$, acting on this charge, drives the system away from equilibrium. Between successive collisions the motion of the moving particle is governed by the equations of motion $\dot{\vec{r}} = \vec{v}, \dot{\vec{v}} = q\vec{E}/m - \alpha\vec{v}, \alpha = q(\vec{E}\cdot\vec{v})/mv^2$, where $\vec{r}$ is the position and $\vec{v}$ the velocity of the particle and $v = (\vec{v})$. Without loss of generality the field $\vec{E} = (0, 0, E)$ is taken to point into the positive z direction. The term $-\alpha\vec{v}$ is a Gaussian thermostatting force designed to maintain a constant kinetic energy $m\vec{v}^2/2$ for the moving particle. These equations are readily integrated [1,6].

Since the collisions are instantaneous and elastic, the position of the moving particle is unaffected by the collision, whereas its velocity changes discontinuously according to

$$\vec{v}_f = \vec{v}_i - 2(\vec{v}_i \cdot \hat{n})\hat{n}\,. \tag{1}$$

Throughout, the subscripts i and f refer to states immediately before or after a collision, respectively. $\hat{n}$ is a unit vector pointing from the center of the scatterer to the collision point.

Consider a reference trajectory in phase space specified by the vector $\vec{\Gamma}(t)$. The time evolution of the system is given by $\vec{\Gamma}(t) = \Phi^t(\vec{\Gamma}(0))$, where Φ^t is the phase flow. An infinitesimal perturbation is specified by a tangent vector $\delta\vec{\Gamma}(0)$ and evolves according to the linearized equation $\delta\vec{\Gamma}(t) = \partial\Phi^t/\partial\vec{\Gamma}\cdot\delta\vec{\Gamma}(0)$. The Lyapunov exponents [7] $\lambda_l = \lim_{t\to\infty}\frac{1}{t}\ln|\delta\vec{\Gamma}_l(t)|/|\delta\vec{\Gamma}_l(0)|$, $l = 1, \dot{s}, L$, measure the exponential growth or decay of L initially orthogonal perturbations in phase space. L is the phase-space dimension. In the three-dimensional Lorentz gas two of the six exponents vanish due to the conservation of kinetic energy and the nonexponential behavior in the flow direction. Thus the Lyapunov spectrum consists of the ordered set of exponents $(\lambda_1^+, \lambda_2^+, 0, 0, \lambda_2^-, \lambda_1^-)$ where, at least for small fields, $\lambda_{1,2}^+ > 0$ and $\lambda_{1,2}^- < 0$.

For the computation of these exponents we recently proposed a generalization [8] of the classical method of Benettin *et al.* [7]. It requires the simultaneous computation of the time evolution of a reference trajectory and of L tangent vectors. Between successive collisions the analytical solution [1,6] is used. These explicit expressions, when differentiated, yield the time evolution of the tangent vectors. When the particle collides with a fixed scatterer, the phase trajectory changes discontinuously according to (1). The corresponding discontinuous change of a tangent vector can be deduced from a general formalism outlined in Ref. [8]. In the following we merely quote the results for an elastic collision of a point particle with a fixed hard sphere.

When the moving particle collides with a scatterer, the positional part $\delta\vec{r}$ of a tangent vector $\delta\vec{\Gamma} = (\delta\vec{r}, \delta\vec{v})$

suffers a specular reflection on the surface of the scatterer:

$$\delta\vec{r}_f = \delta\vec{r}_i - 2(\delta\vec{r}_i \cdot \hat{n})\hat{n}\,. \tag{2}$$

The transformation rule for the velocity components is more involved:

$$\delta\vec{v}_f = \delta\vec{v}_i - 2(\delta\vec{v}_i \cdot \hat{n})\hat{n} + \delta\vec{v}_c + \delta\vec{v}_E\,. \tag{3}$$

In addition to the specular-reflection terms, two other contributions arise in this equation. The third term on the right-hand side, $\delta\vec{v}_c$, is a consequence of the curvature of the scatterer surface. It is explicitly given by

$$\delta\vec{v}_c = -2[(\vec{v}_i \cdot \delta\hat{n})\vec{n} + (\vec{v}_i \cdot \hat{n})\delta\hat{n}], \tag{4}$$

where $\delta\hat{n} \equiv \partial\hat{n}/\delta\vec{r} \cdot \delta\vec{r}_c$ is the variation of the normal vector $\hat{n}$, caused by the variational displacement

$$\delta\vec{r}_c = \delta\vec{r}_i - \frac{(\delta\vec{r}_i \cdot \hat{n})}{(\vec{v}_i \cdot \hat{n})} \tag{5}$$

of the collision point on the surface of the scatterer due to the perturbation. The last term on the right-hand side of (3),

$$\delta\vec{v}_E = \frac{2q}{m}\,(\hat{n} \cdot \vec{E})\,\frac{\delta\vec{q}_i \cdot \hat{n}}{\vec{v}_i \cdot \hat{n}}\left[\hat{n} + \frac{(\vec{v}_i \cdot \hat{n})}{v^2}\,\vec{v}_f\right], \tag{6}$$

is a consequence of the applied field and of the thermostatting force. In combination, Eqs. (2)–(6) enable us to obtain the exact time evolution of any tangent-space vector and, hence, to apply Benettin's method for the computation of the full Lyapunov spectrum.

In our numerical work we measure distances in units of a, time in units of a/v, Lyapunov exponents and collision rates in units of v/a, and the external field in units of mv^2/qa. The number density is defined as $n \equiv N/V$, where N is the number of scatterers and V is the volume of the simulation box. The scatterers are placed at random in a cubic simulation box with periodic boundary conditions. To reduce the computational effort, the simulation box is divided into subcells containing one scatterer on the average. The next collision point of the moving particle with a scatterer or its crossing point with the boundary of the current subcell is determined numerically with an accuracy of 10^{-12}. At each collision the rules (1), and (2), (3) are applied to the reference system and the tangent vectors, respectively. The full set of tangent vectors is periodically reorthonormalized using the Gram-Schmidt method, and the Lyapunov exponents are obtained from the time average of the logarithms of the normalization factors [7].

Let us consider equilibrium systems ($E = 0$) first. Figure 1 shows λ_1^+ and λ_2^+ as a function of the scatterer density n for a system of 10^5 scatterers. The standard deviation of all points is better than 0.15%. The negative exponents are not shown. They may be obtained from the symmetry relations $\lambda_1^+ = -\lambda_1^-$ and $\lambda_2^+ = -\lambda_2^-$,

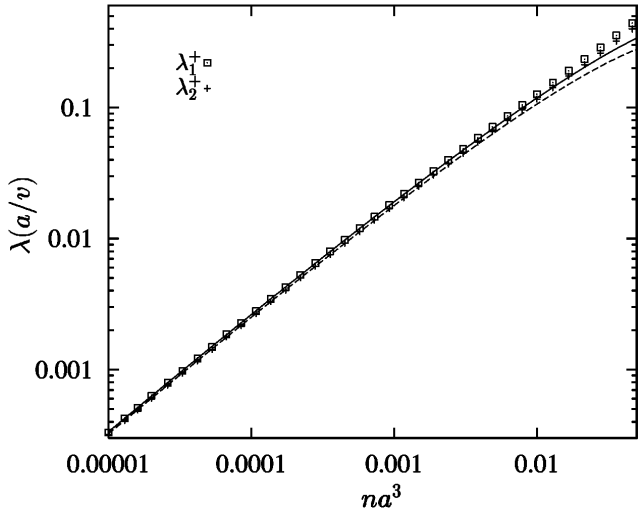

FIG. 1. Lyapunov exponents λ_1^+ (squares) and λ_2^+ (crosses) of the three-dimensional random Lorentz gas in equilibrium as a function of the density n.

which are a consequence of the symplectic nature of the equations of motion for the equilibrium systems [5,9]. The solid line (λ_1^+) and the broken line (λ_2^+) are the kinetic-theory results of Latz, van Beijeren, and Dorfman summarized in Eq. (6) of the accompanying paper [5]. Within the density range accessible to kinetic theory [10], the agreement between our numerical results and the theoretical predictions is excellent. We note that the maximum Lyapunov exponents for two- and three-dimensional systems are very similar if taken as a function of the collision rate.

Next we turn to stationary nonequilibrium systems with a homogeneous field acting on the moving particle. In Fig. 2 we show the deviation of the Lyapunov exponents from their equilibrium value $\Delta\lambda_i^{\pm}(E) \equiv \lambda_i^{\pm}(E) - \lambda_i^{\pm}(0)$ for a density $n = 0.001a^{-3}$ as a function of the square of the field. On the abscissa we use $\tilde{\epsilon}^2/\tilde{n}$, where $\tilde{\epsilon} = qaE/mv^2$ and $\tilde{n} = n\pi a^3$. The corresponding *equilibrium* exponents $\lambda_1^+(0) = -\lambda_1^-(0) = (0.019\,214 \pm 1 \times 10^{-6})v/a$ and $\lambda_2^+(0) = -\lambda_2^-(0) - = (0.018\,034 \pm 1 \times 10^{-6})v/a$ were carefully determined from an average over 100 configurations, each constructed of 2×10^5 scatterers, and a total of 470×10^6 collisions. For the points at finite field the same parameters apply; however, the total number of collisions which could be followed was about 40×10^6 per point. The resulting standard deviation for $\Delta\lambda_i^{\pm}(E)$ is indicated by the error bars in Fig. 2. We defer the discussion of these results and the comparison with theory to the end of the Letter.

For thermostatted nonequilibrium steady-state systems the respective transport coefficient is strictly proportional to the sum of all Lyapunov exponents which, in turn, is proportional to the time-averaged thermostat variable $\langle\alpha\rangle$ [9,11]. For the 3D-Lorentz gas the conductivity $\sigma \equiv q\langle v E\rangle/E^2$, which for small fields is related to the diffusion coefficient D through an Einstein relation, is

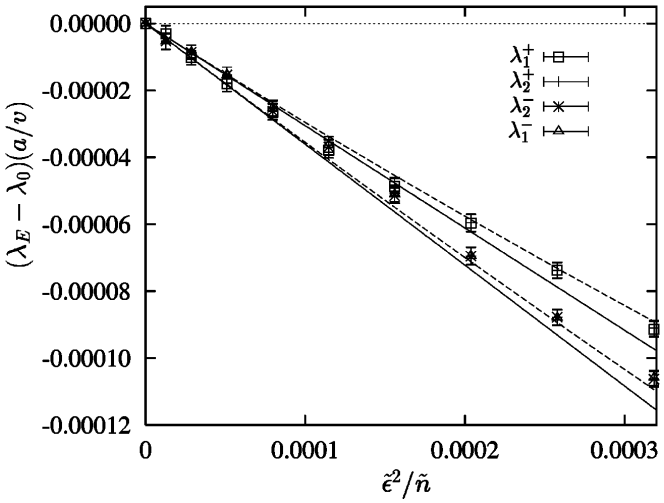

FIG. 2. Deviation of the Lyapunov exponents from their equilibrium value as a function of $\tilde{\epsilon}^2/\tilde{n}$ at a density $n = 0.001a^{-3}$. The solid lines are the theoretical predictions according to Eqs. (13) of Ref. [5]. The broken lines refer to the results obtained with the stochastic technique described in the main text.

given by

$$\sigma = \frac{q^2 D}{kT} = -\frac{mv^2}{2E^2} \sum_i \lambda_i = \frac{2}{3} \frac{q^2 a}{mv\tilde{n}} + O(E^2). \quad (7)$$

The last equality is derived by inserting the kinetic-theory expressions (5) of Ref. [5]. In Fig. 3 the diamonds represent simulation results for the normalized diffusion coefficient $D\tilde{n}/av$ as a function of $\tilde{\epsilon}^2/\tilde{n}$ for the density $n = 0.001a^{-3}$. D was obtained from the conductivity σ via the first equality of (7), and σ was computed from its definition given above, the ratio of the time-averaged current in field direction to the applied field.

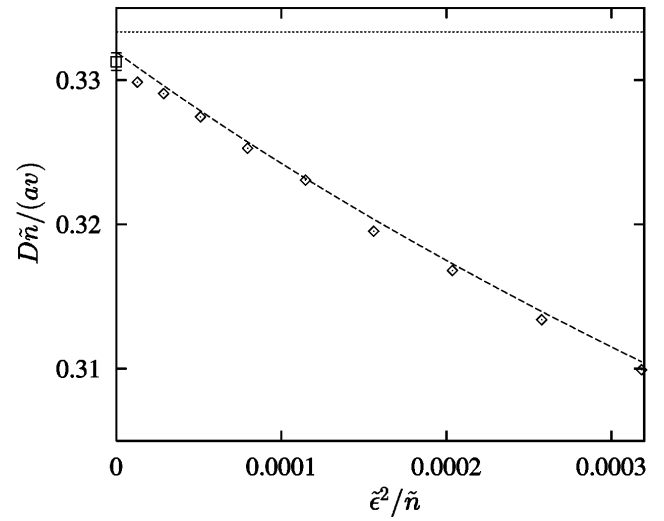

FIG. 3. Dimensionless diffusion coefficient $D\tilde{n}/av$ as a function of $\tilde{\epsilon}^2/\tilde{n}$ at a density $n = 0.001a^{-3}$. The broken line refers to the results obtained with the stochastic technique described in the main text. The square with error bar at $\tilde{\epsilon}^2/\tilde{n} = 0$ is the equilibrium Green-Kubo result.

Alternatively, σ (or D) can be obtained also from the sum of all Lyapunov exponents as indicated by (7). On the scale of Fig. 3 both methods give indistinguishable results. The square with error bar at $\tilde{\epsilon}^2/\tilde{n} = 0$ was obtained under equilibrium conditions from the Green-Kubo relation $D = \int_0^\infty \langle v_x(0) v_x(t)\, dt \rangle$.

The method just described requires the precise localization of the collision points and becomes inefficient for low densities. To overcome this limitation to accuracy in this density regime, we propose a stochastic method (SM), which is, in essence, a numerical method for solving the Boltzmann equation. It is similar to the Monte Carlo methods for the simulation of neutron transport in random media [12] and the direct simulation Monte Carlo method [13]. The main idea is that the streaming motion and the collisions are uncoupled for low-enough densities, for which correlations of subsequent collisions are negligible. The dynamics of the system is modeled by appropriate probability distributions of the collision parameters and of the collision time.

The SM proceeds as follows. (a) The velocity of the moving particle is initialized with random orientation. Since the streaming motion and the collisions are uncoupled, the particle position is irrelevant and need not be followed in time. (b) A collision time τ is drawn from the distribution $p(\tau) = \nu \exp(-\nu\tau)$, where ν is the collision rate. ν or, equivalently, the mean free path, is an input parameter for the simulation. This exponential distribution is a consequence of the random scatterer configuration and may be derived from the probability of a random event to occur after a time t. (c) The velocity of the moving particle is advanced for τ yielding $\vec{v}_i$ for the next collision. Also the tangent vectors are updated accordingly. (d) The velocity vector and the tangent vectors are subjected to a random collision. Since a collision with a hard sphere is isotropic, the direction of $\vec{v}_f$ is uniformly distributed over a sphere of radius v. From $\vec{v}_i$ and $\vec{v}_f$ the unit vector $\hat{n}$ is determined, and the transformation rules (2) and (3) are applied to all tangent vectors. (e) The steps (b)-(d) are repeated until the desired number of collisions is reached. It should be noted that, although the time evolution of the reference system is determined by stochastic events, tangent-space dynamics is completely deterministic.

We tested SM for the same density $n = 0.001a^{-3}$ as was used before. It corresponds to a mean free path $l = 317.0a$. For each field 4×10^8 collisions were computed. The positive equilibrium exponents obtained with this method, $\lambda^+(0) = (0.019\,197 \pm 1 \times 10^{-6})v/a$ and $\lambda^+(0) = (0.018020 \pm 1 \times 10^{-6})v/a$, differ from the numbers quoted above by $\sim 0.1\%$. This discrepancy is an indication of the systematic errors at this density due to the statistical assumptions for the stochastic method. However, even this small error cancels to a large extent if the difference $\Delta\lambda_i^\pm(E) \equiv \lambda_i^\pm(E) - \lambda_i^\pm(0)$ is computed, as is the case shown in Fig. 2. All points for 20 different fields are on top of two smooth dashed lines shown in the figure for clarity. They do not show any noticeable scatter

with respect to these curves on the scale of the figure. This lack of scatter is achieved only if the *same* sequence of random numbers is used for the computation of $\lambda_i^{\pm}(E)$ and $\lambda_i^{\pm}(0)$. The statistical fluctuations are effectively reduced by the difference. The convergence of $\Delta\lambda_i^{\pm}(E)$ to their asymptotic values is about 100 times faster than with a computation using different sequences of random numbers.

We find very good agreement in Fig. 2 for the results of the stochastic method (dashed curves) for $\Delta\lambda_i^{\pm}(E)$ with the points obtained with the more conventional algorithm discussed before. The same is true also for the reduced diffusion coefficient as a function of the squared field in Fig. 3, where the dashed curve (*no fit*) again refers to the results of SM.

The field dependence of the two positive Lyapunov exponents is numerically found to be identical including terms to at least fourth order in the field, as is obvious from the upper dashed curve in Fig. 2 which contains the points for $\Delta\lambda_{1,2}^{\pm}(E)$. Likewise, the field dependence of the two negative exponents is also identical and is depicted by the lower dashed curve in the figure. The solid lines are the kinetic-theory results predicted by Eq. (6) of the preceding Letter [5]. According to this theory accurate to second order in the field, the two positive and the two negative exponents have the same field dependence. This is in agreement with our experimental results. Furthermore, the slopes of the theoretical curves are in perfect agreement with our SM-simulation results in the vanishing-field limit.

Two remarks are in order: First, the negative exponents vary more strongly with the square of the field than the positive exponents. This is in contrast to the two-dimensional Lorentz gas, for which the (single) positive exponent varies more strongly with E^2 than the (single) negative [4]. Second, deviations from the quadratic field dependence are observed in Fig. 2. They indicate that contributions of $O(E^4)$ to the Lyapunov exponents become important already for such small fields as are included in the range of the figure.

Finally, we compare our simulation results for the diffusion coefficient with the predictions of the kinetic theory. According to Eq. (5) of Ref. [5] a field-independent constant for $D\tilde{n}$ is obtained, indicated by the dotted horizontal line in Fig. 3. The slope of our numerical data points to the significance of $O(E^4)$ terms in the sum of all Lyapunov exponents not included in the theory. Furthermore, the small discrepancy of less than 1% for vanishing field is due to the omission of higher-order terms of the form $\tilde{n} + b\tilde{n}^2 \ln\tilde{n}$ by the theory. Introduction of the next-order correction known, however, only for the random Lorentz gas with scatterer overlap permitted [14], reduces this discrepancy to about 0.5%.

We conclude by stressing again the remarkable agreement of our numerical results with the theoretical predictions of [5]. We have shown that the accuracy obtainable by deterministic and stochastic simulation techniques allows detailed numerical predictions for all field-dependent Lyapunov exponents of the random Lorentz gas. The development of a very efficient stochastic method makes also very low-density systems accessible to simulation. Similar techniques have been used recently also for the study of many-body hard-disk and hard-sphere [15] systems in two and three dimensions, respectively.

We would like to thank Professor H. v. Beijeren, Professor J. R. Dorfman, Dr. A. Latz, and Professor W. G. Hoover for stimulating discussions and cooperation on this and related work. The authors gratefully acknowledge the financial support from the *Fonds zur Förderung der wissenschaftlichen Forschung*, Grant No. P09677, and the generous allocation of computer resources by the Computer Center of the University of Vienna.

[1] B. Moran and W. G. Hoover, J. Stat. Phys. **48**, 709 (1987).
[2] Ch. Dellago, L. Glatz, and H. A. Posch, Phys. Rev. E **52**, 4817 (1995).
[3] H. van Beijeren and J. R. Dorfman, Phys. Rev. Lett. **74**, 1319 (1995).
[4] H. van Beijeren, J. R. Dorfman, E. G. D. Cohen, H. A. Posch, and Ch. Dellago, Phys. Rev. Lett. **77**, 1974 (1996).
[5] A. Latz, J. R. Dorfman, and H. van Beijeren, preceding Letter, Phys. Rev. Lett. **78**, 207 (1997).
[6] C. P. Dettmann, G. P. Morriss, and L. Rondoni, Phys. Rev. E **52**, R5746 (1995).
[7] G. Benett, in L. Galgani, A. Giorgilli, and J.-M. Strelcyn, Meccanica **15**, 9 (1980); A. Wolf, J. B. Swift, H. L. Swinney, and J. A. Vastano, Physica (Amsterdam) **16D**, 285 (1985).
[8] Ch. Dellago, H. A. Posch, and W. G. Hoover, Phys. Rev. E **53**, 1485 (1996).
[9] H. A. Posch and W. G. Hoover, Phys. Rev. A **38**, 473 (1988).
[10] Ch. Dellago and H. A. Posch, Phys. Rev. E (to be published).
[11] H. A. Posch and W. G. Hoover, Phys. Rev. A **39**, 2175 (1989).
[12] M. H. Kalos and P. A. Whitlock, *Monte Carlo Methods: Basics* (John Wiley and Sons, New York, 1986), Vol. 1.
[13] G. A. Bird, Phys. Fluids **6**, 1518 (1963); G. A. Bird, *Molecular Gas Dynamics and the Direct Simulation of Gas Flows*, Oxford Engineering Science Series Vol. 42 (Clarendon Press, Oxford, 1994).
[14] C. Bruin, Physica **72**, 261 (1974); A. Weyland and J. M. J. Van Leeuwen, Physica **38**, 35 (1968).
[15] Ch. Dellago and H. A. Posch, Physica D (to be published).